Cardiovascular Applications of Photon-Counting CT: When Cardiac CT Meets Cardiac MR

Adrien De Minteguiaga, M.D.; Benjamin Longère, M.D., Ph.D.; Christos Gkizas, M.D., Ph.D.; Aimée Rodriguez Musso, M.D.; Mehdi Haidar, M.D.; François Pontana, M.D., Ph.D.

CHU Lille, Department of Cardiothoracic Radiology, Lille, France

Background

Cardiac magnetic resonance imaging (CMR) is now well established as the reference non-invasive modality for the assessment of heart diseases, particularly owing to its ability to characterize the myocardium [1]. Nevertheless, CMR suffers from an extensive acquisition time that may be difficult to handle for patients with cardiac conditions. In clinical routine it typically relies on two-dimensional 5–8 mm thick slices with interslice gaps of up to 20%. Computed tomography (CT) has recently undergone a paradigm shift in detector technology with the advent of photon-counting detectors [2]. With the NAEOTOM Alpha family (Siemens Healthineers, Forchheim, Germany) a photon-counting CT (PCCT) CT generation is made available. Early evaluations of this new generation of detectors have opened the way to PCCT-based myocardial tissue characterization and functional imaging, providing information comparable to that obtained with CMR.

Photon-counting technology

Limitations of energy-integrating detectors

Conventional CT systems are equipped with energy-integrating detectors (EIDs), which indirectly convert X-rays into an electrical signal. In this process, incoming X-rays are first converted into visible light within a scintillator, with light intensity proportional to the X-ray energy. The emitted light is then converted into an electrical signal by a photodiode, with signal intensity proportional to the amount of visible light. To prevent optical crosstalk between adjacent detector elements, blind septa must be interposed, which limits the achievable in-plane spatial resolution and/or reduces the effective surface, especially for very fine pixelations. This indirect detection chain is also prone to increased electronic noise at low X-ray energies, and the resulting electrical signal represents an integrated sum of the entire detected X-ray spectrum over the projection time measurement [3].

Benefits of photon-counting detectors

By contrast, photon-counting detectors (PCDs) directly convert X-ray photons into electrical signals using semiconductor technology. Each incoming photon deposits its energy into the semiconductor, ejecting an electron that is attracted to a pixelated anode under a strong electric field. This generates an electrical pulse, the amplitude of which is proportional to the photon's energy.

Improved spatial resolution: The pixelated anode design eliminates the need for blind septa, thereby enhancing the intrinsic in-plane spatial resolution. Each anode pixel can be subdivided into smaller sub-elements that can be individually processed to achieve ultra-high in-plane resolution. Every photon interaction is individually detected and processed according to its energy, which constitutes the core of the photon-counting principle [4].

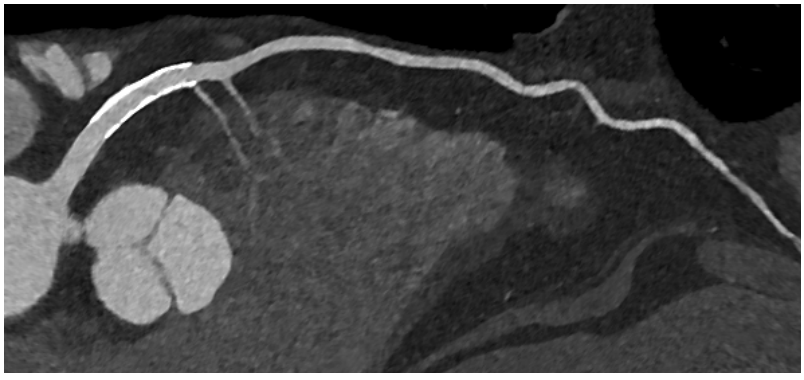

1 Stent patency assessment in a 73-year-old man. Ultra-high-resolution coronary CT angiography ($0.11 \times 0.11 \times 0.2$ mm^3; Bv56 kernel; 768×768 matrix) of the left anterior descending artery. Stent patency is clearly assessed without blooming artifacts. Note the good delineation of two septal branches.

Noise reduction: During signal processing, energy thresholds are applied to exclude electronic noise through a binning process. In contrast to an EID detector system, PCD's can filter out unwarranted/non-event-related signals. This is also one of the reasons why PCCT systems are superior to EID systems in terms of radiation-dose efficiency.

Spectral data without compromising temporal resolution: Additional higher-energy thresholds can be applied to create multiple energy bins, classifying detected photons according to their energy level. For clinical applications, data from higher and lower energies are required. Therefore, during further data management, two bins representing these energy levels are generated and used for further image reconstruction/data analysis. In dual-source dual-energy CT acquisitions, spectral separation is achieved by applying two different mean energies with the spectrum emitted from the X-ray tube (e.g., a tube voltage of 70 kVp and Sn140 kVp), which reduces the in-plane temporal resolution. By contrast, PCCT intrinsically achieves spectral decomposition at the detector level. Consequently, both tube-detector pairs contribute to spectral data acquisition, preserving high temporal resolution without sacrificing spectral information.

Coronary artery disease

Coronary CT angiography is now well established as the first line imaging modality for patients with symptoms suggestive of chronic obstructive coronary artery disease [5]. However, functional testing is generally preferred over anatomical assessment in patients with coronary stents. The ultra-high spatial resolution provided by PCCT enables substantial improvements in diagnostic confidence in assessing coronary stent patency (Fig. 1, Fig. 2) as well as in patients with high calcified plaque burden [6]. PCCT has also shown to reduce beam-hardening artifacts.

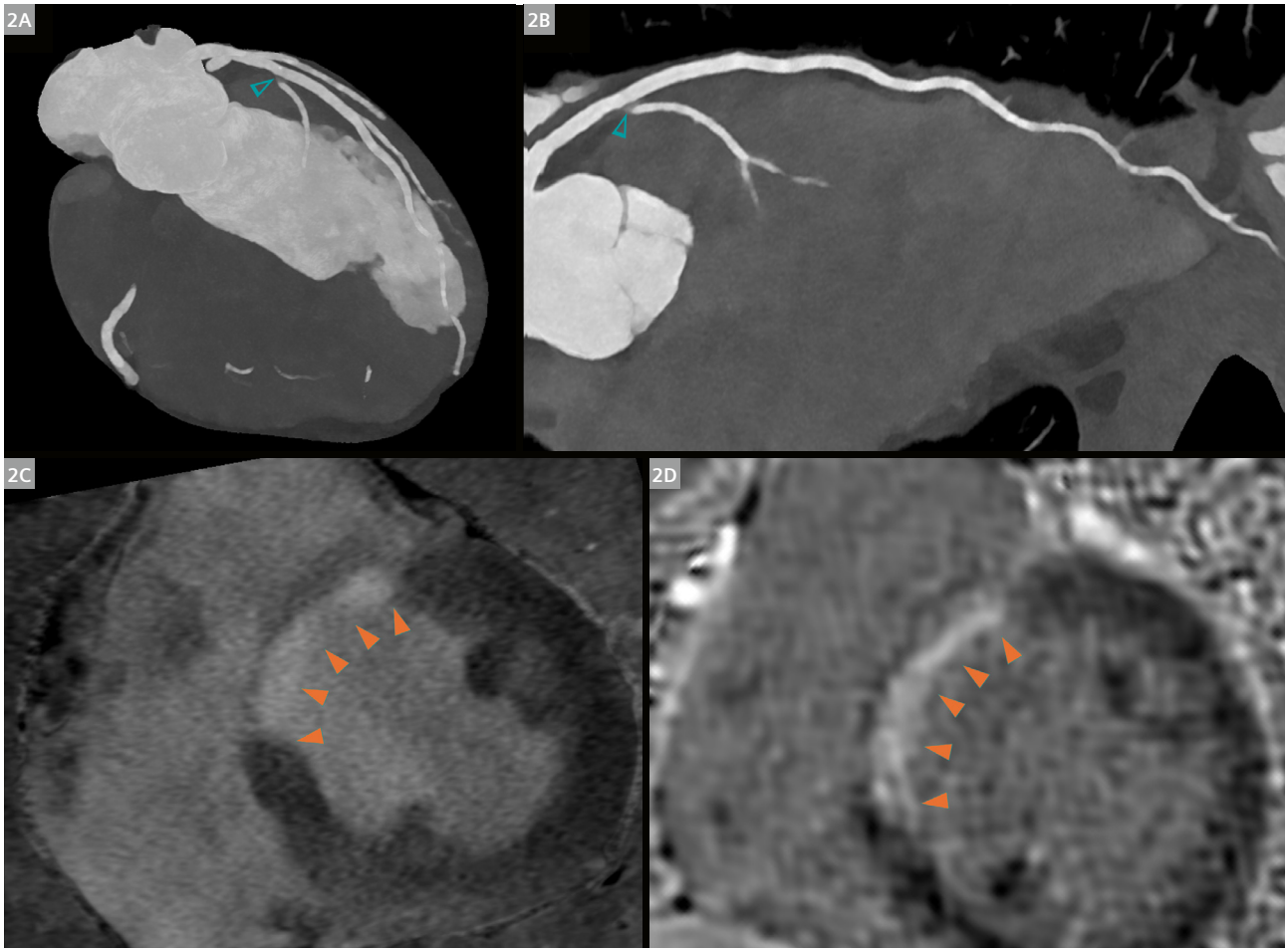

2 34-year-old male patient with a history of drug use, referred for suspected acute myocarditis in the context of viral infection. **(2A, 2B)** Maximum intensity projection reconstructions showing ostial stenosis of the first septal branch arising from the left anterior descending artery (hollow arrowhead), likely related to cocaine-induced vasospasm. **(2C)** Iodine map reconstruction from the photon-counting CT-MDE acquisition and **(2D)** late gadolinium enhancement CMR image showing subendocardial enhancement of the mid-anterior septal wall (solid arrowheads).

Beyond volumetric measurements, the main historical advantage of CMR lies in its ability to detect and quantify myocardial fibrosis through late gadolinium enhancement (LGE), which has demonstrated strong prognostic value in the management of myocardial infarction [7, 8]. The feasibility of CT-based myocardial delayed enhancement (CT-MDE) has also been established using conventional EID systems, with reported radiation doses ranging from 0.5–7 mSv for polychromatic acquisitions, and from 2.2–4.7 mSv for dual-energy acquisitions. However, low-dose polychromatic protocols have shown limited image quality, particularly in larger patients [9]. Using spectral reconstructions such as low-energy monoenergetic imaging or iodine maps, PCCT improves the depiction of myocardial infarction on CT myocardial delayed enhancement (MDE) images (Fig. 2), while achieving approximately 1 mSv for full three-dimensional cardiac coverage [10, 11].

However, the hemodynamic significance of an obstructive coronary artery lesion cannot be determined from anatomical findings alone, as up to half of anatomically obstructive plaques show no lesion-specific ischemia on downstream functional testing [12]. Stress CT myocardial perfusion imaging has been shown to improve the specificity of coronary CT angiography [13]. The feasibility of PCCT-based myocardial perfusion imaging has recently been demonstrated (Fig. 3), with excellent diagnostic accuracy compared with functional reference standards such as stress CMR [14].

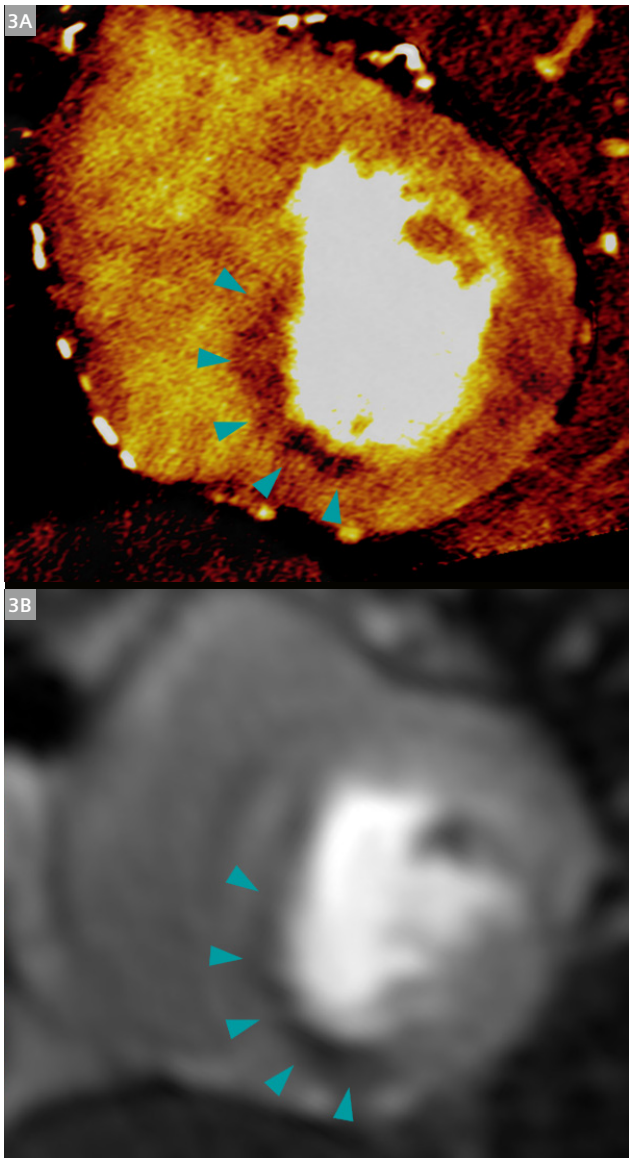

3 55-year-old female patient with a history of coronary artery bypass graft and new-onset exertional chest pain. **(3A)** Stress photon-counting CT myocardial perfusion imaging showing a subendocardial perfusion defect in the mid-inferior septal wall (arrowheads). **(3B)** Corresponding perfusion defect confirmed on stress CMR.

Myocardial characterization

A major strength of CMR lies in its well-established ability to characterize myocardial tissue, particularly through techniques such as parametric mapping and extracellular volume (ECV) quantification [15]. However, CMR-derived ECV requires acquisition of both native and post-contrast T1 maps, typically separated by 20–30 minutes, which may introduce misregistration and consequently bias the ECV calculation [15]. Dual-energy CT can overcome this technical limitation by generating an iodine map from a single scan [10]. Thanks to their dual-source architecture and photon-counting detector technology, the NAEOTOM Alpha.Peak and Pro acquire spectral data with high-temporal resolution. The ECV values derived from CMR and PCCT have been compared in patients with acute myocarditis (Fig. 4) or hypertrophic cardiomyopathies, showing no significant differences between modalities, with mean errors around 0.5% and narrow limits of agreement [16, 17]. Moreover, in patients with hypertrophic cardiomyopathy (Fig. 5), a PCCT-derived ECV cut-off value of 33.4% has been demonstrated to accurately identify patients with LGE ≥ 15% on CMR. This threshold can be considered in the decision-making process for prophylactic placement of an implantable cardioverter-defibrillator[1] [17, 18].

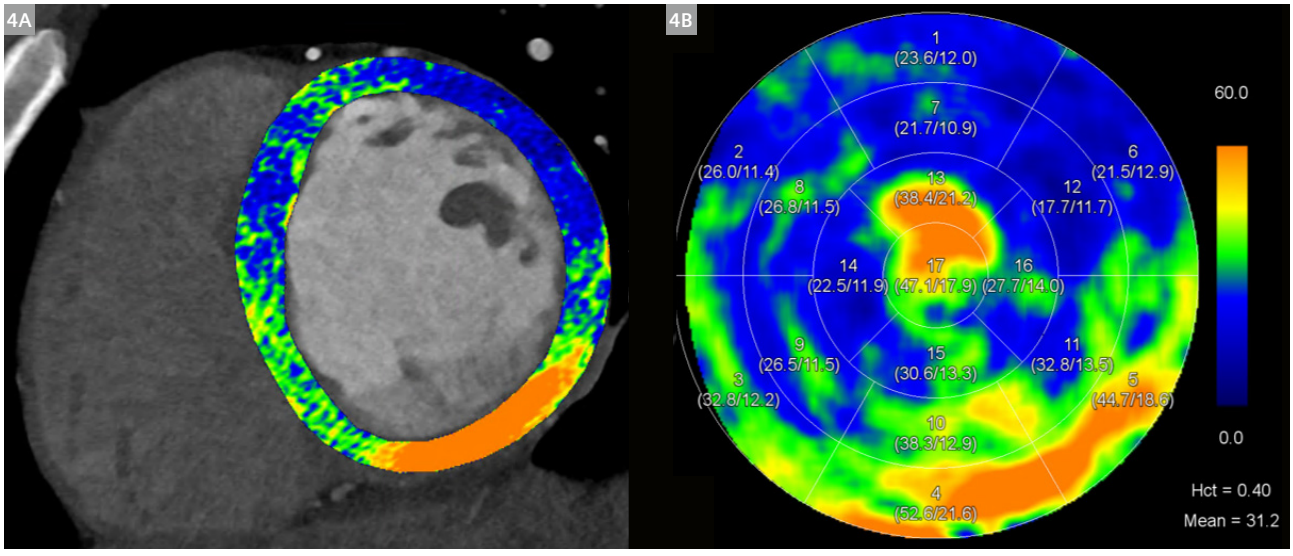

4 18-year-old male patient with acute chest pain in the context of SARS-CoV2 infection. **(4A)** Photon-counting CT-derived extracellular volume map overlay derived from myocardial late enhancement. **(4B)** Extracellular volume polar map derived from photon-counting CT.

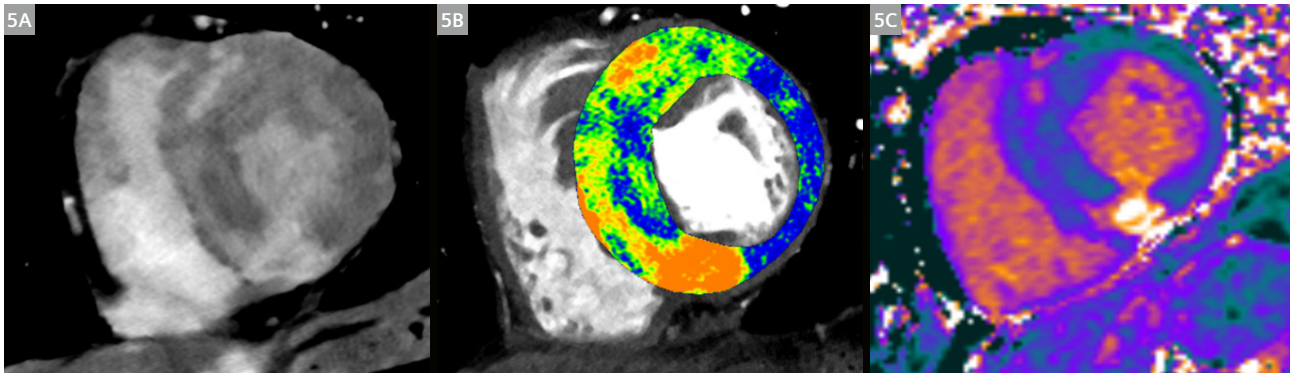

5 69-year-old female patient without history of high blood pressure, referred for evaluation of obstructive coronary heart disease in the context of new-onset dyspnea. **(5A)** Photon-counting CT shows left ventricular hypertrophy with intramyocardial fibrotic lesion on MDE series. **(5B)** Extracellular volume map overlay derived from photon-counting CT. **(5C)** Extracellular volume map calculated from CMR.

[1] *The MRI restrictions (if any) of the metal implant must be considered prior to patient undergoing MRI exam. MR imaging of patients with metallic implants brings specific risks. However, certain implants are approved by the governing regulatory bodies to be MR conditionally safe. For such implants, the previously mentioned warning may not be applicable. Please contact the implant manufacturer for the specific conditional information. The conditions for MR safety are the responsibility of the implant manufacturer, not of Siemens Healthineers.*

Heart valve disease

Advanced imaging modalities such as three-dimensional echocardiography, CMR, and cardiac CT have become central to the assessment of patients with valvular heart disease [19]. In this clinical context, cardiac CT and CMR are highly complementary. Cardiac CT provides a comprehensive assessment of cardiac and vascular anatomy, including evaluation of peripheral arterial calcification, plaque burden, and annular measurements, which are essential for patient eligibility and procedural planning in heart valve interventions. CMR, on the other hand, remains the reference standard for quantifying ventricular volumes and function, as well as regurgitant volumes or myocardial fibrosis. After heart valve intervention, cardiac CT plays a key role in the evaluation of suspected prosthetic valve dysfunction. CMR can quantify perivalvular leaks and assess increases in transvalvular gradients, but metal artifacts often limit visualization of prosthetic leaflets (Fig. 6). The ultra-high-resolution acquisition and preserved contrast at high tube voltage achieved with PCCT allow for a substantial reduction of beam-hardening and blooming artifacts [20]. This facilitates visualization of hypoattenuating structures adjacent to the leaflets or annulus – such as thrombus, pannus, or vegetations.

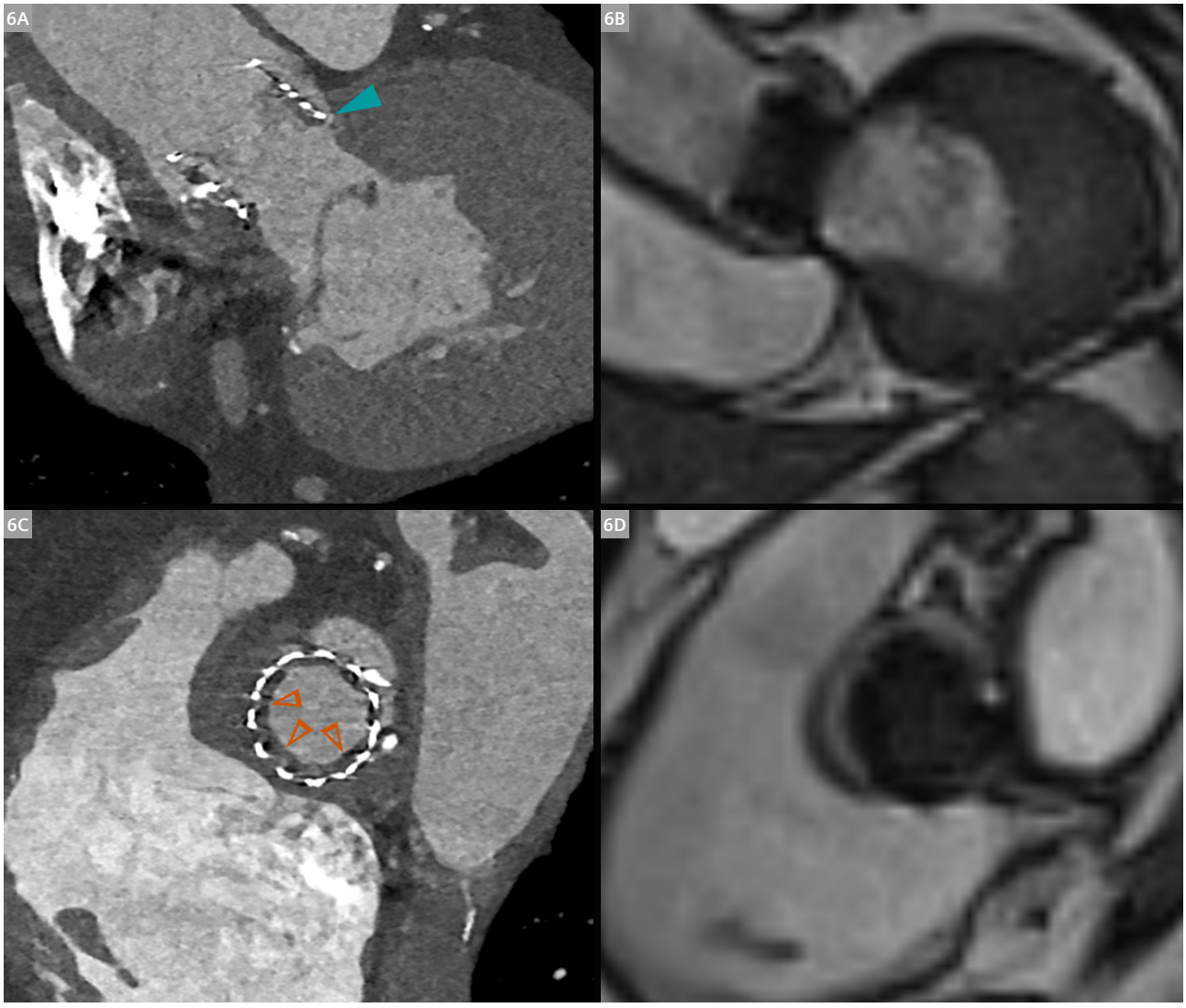

6 78-year-old male patient with a history of transcatheter aortic valve replacement, referred for increased transvalvular gradient detected on transthoracic echocardiography, with suspected periprosthetic regurgitation. **(6A)** Ultra-high-resolution photon-counting CT acquisition demonstrating the paravalvular defect responsible for the regurgitation. **(6B)** CMR accurately quantified the paravalvular leak, but morphological assessment of the prosthetic valve was not feasible due to metal artifacts. **(6C)** Ultra-high-resolution photon-counting CT image showing a circular hypoattenuation within the stent annulus, which could not be assessed on **(6D)** CMR because of susceptibility artifacts.

Flow imaging

Through two-dimensional phase-contrast and four-dimensional flow imaging, CMR is a key modality for evaluating cardiac chamber hemodynamics, especially in patients with poor transthoracic echocardiographic windows [21, 22]. Quantification of regurgitation or intracardiac shunts on CT relies on systolic and diastolic ventricular segmentation, at the cost of increased radiation exposure. An appropriate iodine contrast injection protocol and accurate triggering of the CT acquisition can qualitatively depict intracardiac shunts or leaks. Compared to the materials regularly used in EID systems, the high responsivity of PCDs to low-energy X-ray photons facilitates the visualization of subtle attenuation differences. This is further enhanced by low-keV monoenergetic reconstructions and potentially further improved for the reader by the use of color look-up tables (Fig. 7, Fig. 8) [23].

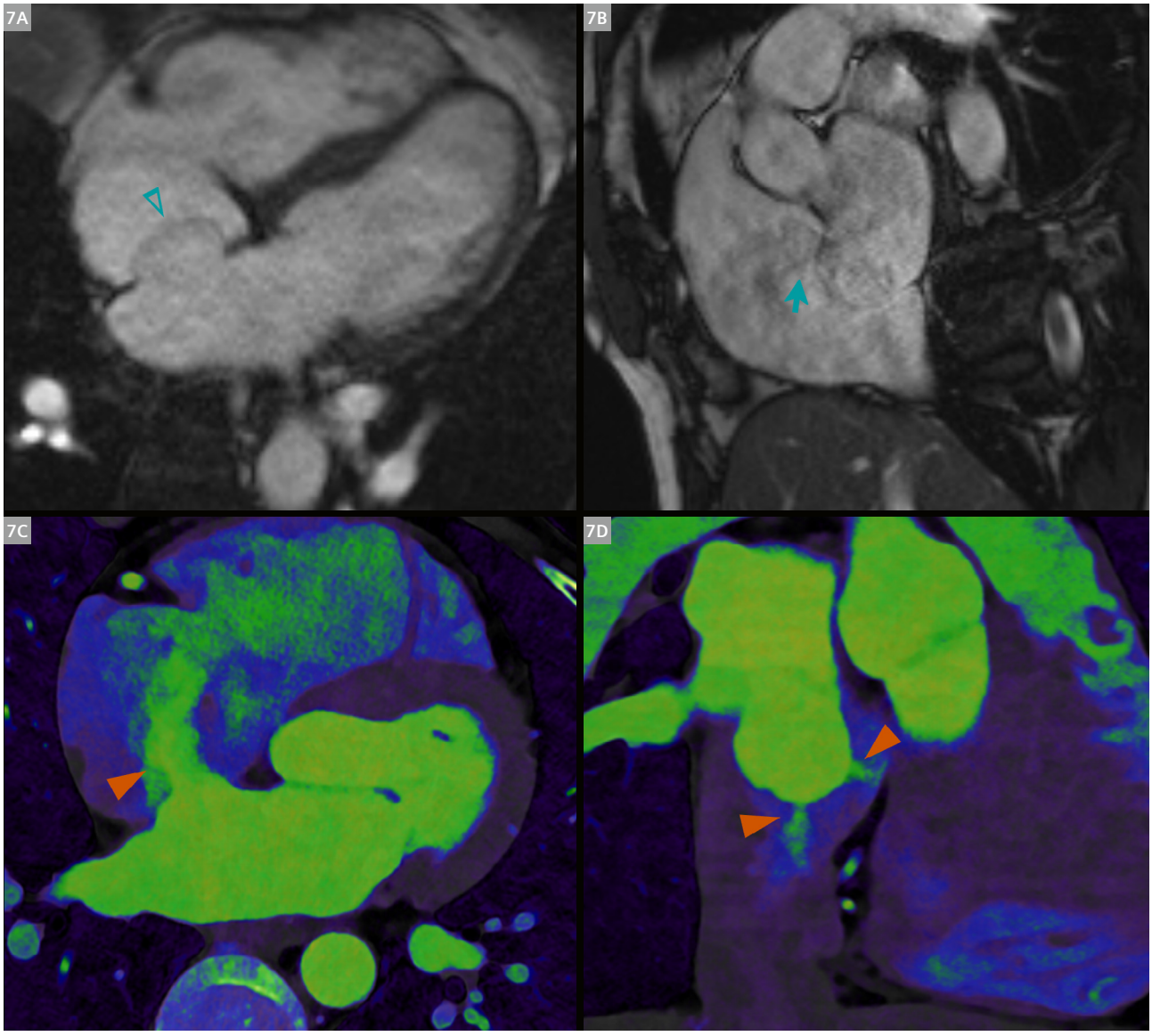

7 39-year-old male patient referred for right-ventricular dilatation. **(7A)** CMR demonstrates an aneurysm of the interatrial septum in the four-chamber view (hollow arrowhead) with **(7B)** interatrial communication visualized as a flow void on the short-axis view (arrow). The Qp/Qs ratio is 1.7. **(7C)** Iodine map derived from photon-counting CT confirms a large interatrial communication on the four-chamber view (arrowhead). **(7D)** Two additional small interatrial communications are identified on the paraseptal right ventricular two-chamber view.

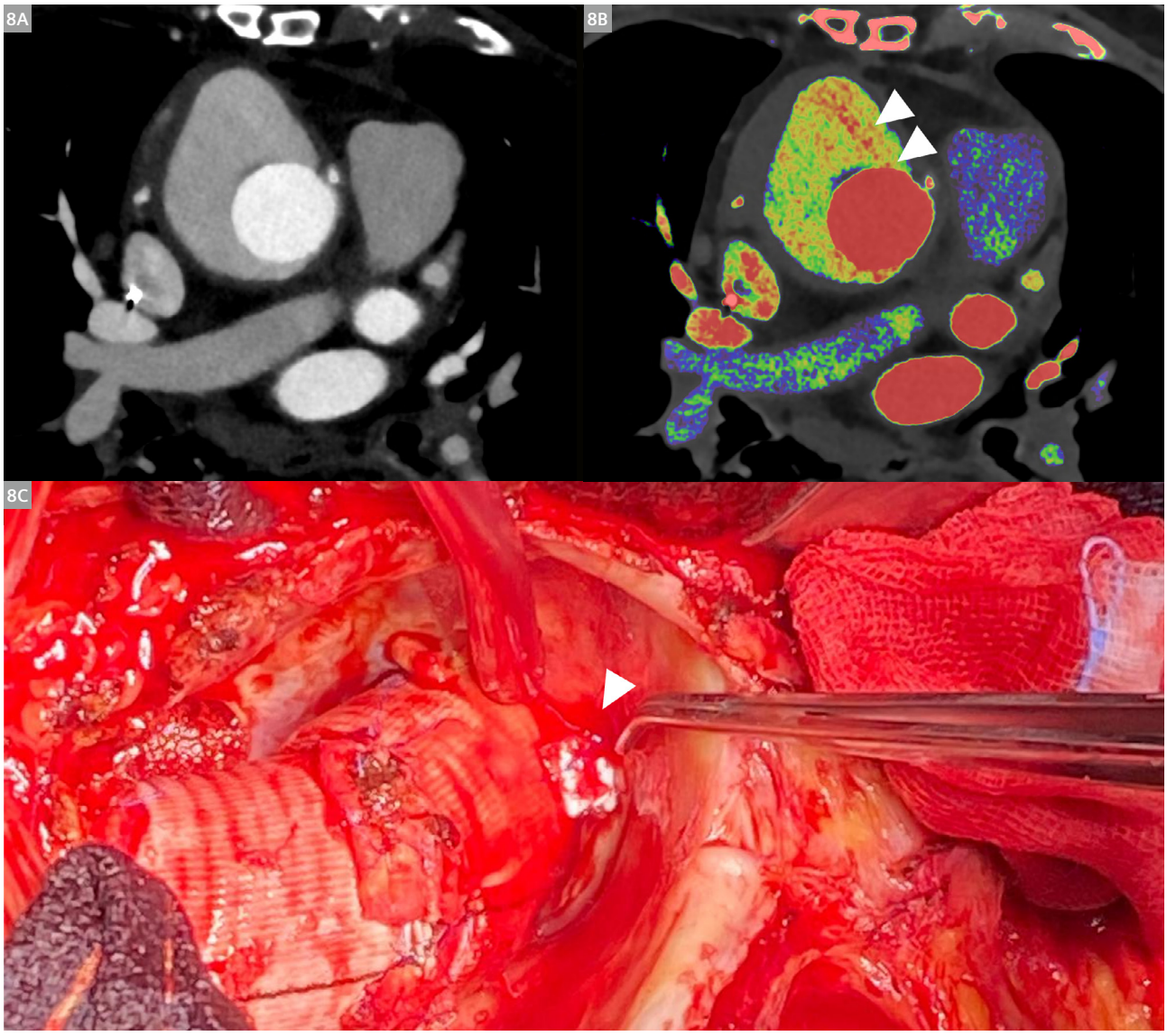

8 88-year-old male patient with a history of ascending aortic replacement, referred for chest pain. (8A) Photon-counting CT angiography of the aorta shows a periaortic hematoma (70 keV monoenergetic reconstruction; 120 kVp conventional-like image). The bleeding source responsible for this hematoma is not confidently identified. (8B) Iodine map overlay using a color look-up table demonstrates the attenuation gradient and precisely locates the bleeding site. (8C) Surgical confirmation of the bleeding origin.
Courtesy of Natacha Rousse, M.D., Heart and Lung Institute, CHU Lille, France.

Conclusion

Photon-counting CT (PCCT) represents a major step toward bridging the historical gap between cardiac CT and CMR. Its ability to provide high-resolution anatomical imaging, quantitative spectral data, and myocardial tissue characterization within a single, time-efficient acquisition brings cardiac CT closer to the comprehensive diagnostic capability traditionally reserved for CMR. However, these modalities should not be seen as competing but as highly complementary. CMR remains the reference standard for advanced tissue characterization, myocardial fibrosis assessment, and complex flow quantification, while PCCT offers unparalleled spatial resolution, reduced acquisition times, and simultaneous evaluation of coronary arteries, myocardium, and valves. Together, PCCT and CMR form a synergistic imaging approach, combining structural and functional insights to refine diagnosis, guide management, and ultimately improve patient care in cardiovascular disease.

References

1 Leiner T, Bogaert J, Friedrich MG, Mohiaddin R, Muthurangu V, Myerson S, et al. SCMR Position Paper (2020) on clinical indications for cardiovascular magnetic resonance. J Cardiovasc Magn Reson. 2020;22(1):76.
2 Willemink MJ, Persson M, Pourmorteza A, Pelc NJ, Fleischmann D. Photon-counting CT: Technical Principles and Clinical Prospects. Radiology. 2018;289:293–312.
3 Flohr T, Schmidt B. Technical Basics and Clinical Benefits of Photon-Counting CT. Invest Radiol. 2023;58(7):441–450.
4 Flohr T, Petersilka M, Henning A, Ulzheimer S, Ferda J, Schmidt B. Photon-counting CT review. Phys Med. 2020;79:126–136.
5 Vrints C, Andreotti F, Koskinas KC, Rossello X, Adamo M, Ainslie J, et al. 2024 ESC Guidelines for the management of chronic coronary syndromes. Eur Heart J. 2024;45(36):3415–3537.
6 Eberhard M, Candreva A, Rajagopal R, Mergen V, Sartoretti T, Stähli BE, et al. Coronary Stenosis Quantification With Ultra-High-Resolution Photon-Counting Detector CT Angiography: Comparison With 3D Quantitative Coronary Angiography. JACC Cardiovasc Imaging. 2024;17(3):342–344.
7 Kim RJ, Fieno DS, Parrish TB, Harris K, Chen EL, Simonetti O, et al. Relationship of MRI delayed contrast enhancement to irreversible injury, infarct age, and contractile function. Circulation. 1999;100(19):1992–2002.
8 Kim RJ, Wu E, Rafael A, Chen EL, Parker MA, Simonetti O, et al. The use of contrast-enhanced magnetic resonance imaging to identify reversible myocardial dysfunction. N Engl J Med. 2000;343(20):1445–53.
9 Rodriguez-Granillo GA. Delayed enhancement cardiac computed tomography for the assessment of myocardial infarction: from bench to bedside. Cardiovasc Diagn Ther. 2017;7(2):159–170.
10 Oyama-Manabe N, Oda S, Ohta Y, Takagi H, Kitagawa K, Jinzaki M. Myocardial late enhancement and extracellular volume with single-energy, dual-energy, and photon-counting computed tomography. J Cardiovasc Comput Tomogr. 2024;18(1):3–10.
11 Mergen V, Sartoretti T, Klotz E, Schmidt B, Jungblut L, Higashigaito K, et al. Extracellular Volume Quantification With Cardiac Late Enhancement Scanning Using Dual-Source Photon-Counting Detector CT. Invest Radiol. 2022;57(6):406–11.
12 Soschynski M, Storelli R, Birkemeyer C, Hagar MT, Faby S, Schwemmer C, et al. CT Myocardial Üerfusion and CT-FFR versus Invasive FFR for Hemodynamic Relevance of Coronary Artery Disease. Radiology. 2024;312(2):e233234.
13 Pontone G, Mushtaq S, Narula J. Dynamic Perfusion with CT Angiography: Adding Another Feather to a Heavily Decorated Cap. J Am Coll Cardiol. 2021;78(20):1950–1953.
14 Longère B, Caseneuve H, Gkizas C, Rodriguez Musso A, Tregubova M, Croisille C, et al. Feasibility of stress myocardial perfusion imaging with photon-counting CT: Initial validation against reference modalities. Diagn Interv Imaging. 2025. Ahead of print. DOI: 10.1016/j.diii.2025.10.005
15 Messroghli DR, Moon JC, Ferreira VM, Grosse-Wortmann L, He T, Kellman P, et al. Clinical recommendations for cardiovascular magnetic resonance mapping of T1, T2, T2* and extracellular volume: A consensus statement by the Society for Cardiovascular Magnetic Resonance (SCMR) endorsed by the European Association for Cardiovascular Imaging (EACVI). J Cardiovasc Magn Reson. 2017;19(1):75.
16 Gkizas C, Longère B, Sliwicka O, Musso AR, Lemesle G, Croisille C, et al. Photon-counting CT-derived extracellular volume in acute myocarditis: Comparison with cardiac MRI. Diagn Interv Imaging. 2025;106(7–8):255–263.
17 Gkizas C, Longère B, Bechrouri S, Ridon H, Musso AR, Haidar M, et al. Photon-counting CT myocardial extracellular volume: A non-invasive biomarker for fibrosis in patients with hypertrophic cardiomyopathy. Diagn Interv Imaging. 2025:S2211–5684(25)00164–0.
18 Arbelo E, Protonotarios A, Gimeno JR, Arbustini E, Barriales-Villa R, Basso C, et al. 2023 ESC Guidelines for the management of cardiomyopathies. Eur Heart J. 2023;44(37):3503–3626.
19 Praz F, Borger MA, Lanz J, Marin-Cuartas M, Abreu A, Adamo M, et al. 2025 ESC/EACTS Guidelines for the management of valvular heart disease. Eur Heart J. 2025:ehaf194.
20 Cademartiri F, Meloni A, Pistoia L, Degiorgi G, Clemente A, Gori CD, et al. Dual-Source Photon-Counting Computed Tomography-Part I: Clinical Overview of Cardiac CT and Coronary CT Angiography Applications. J Clin Med. 2023;12(11):3627.
21 Horowitz MJ, Kupsky DF, El-Said HG, Alshawabkeh L, Kligerman SJ, Hsiao A. 4D Flow MRI Quantification of Congenital Shunts: Comparison to Invasive Catheterization. Radiol Cardiothorac Imaging. 2021;3(2):e200446.
22 Aquaro GD, Barison A, Todiere G, Festa P, Ait-Ali L, Lombardi M, et al. Cardiac magnetic resonance 'virtual catheterization' for the quantification of valvular regurgitations and cardiac shunt. J Cardiovasc Med (Hagerstown). 2015;16(10):663–70.
23 Janin-Manificat A, Sigovan M, Davila E, de Bourguignon C, Si-Mohamed S, Boussel L, et al. Spectral Computed Tomography for the Detection and Characterization of Communications Between the True and the False Lumen in Aortic Dissections. Invest Radiol. 2025. Epub ahead of print.

Professor François Pontana, M.D., Ph.D.
Department of Cardiothoracic Radiology
CHU Lille, Heart and Lung Institute
Boulevard du Professeur Jules Leclercq
59037 Lille Cedex
France
francois.pontana@chu-lille.fr

Contact

Associate Professor Benjamin Longère, M.D., Ph.D.
Department of Cardiothoracic Radiology
CHU Lille, Heart and Lung Institute
Boulevard du Professeur Jules Leclercq
59037 Lille Cedex
France
Benjamin.LONGERE@chu-lille.fr